Charge Transfer Regulated by Domain Differences between Host and Guest Donors in Ternary Organic Solar Cells

Ming-Yang Li,[a] Yue Ren, [a] Jiu-Chang Huang,[a] Ming-Yue Sui,[a] Guang-Yan Sun*[a,b] and Zhong-Min Su*[a,c]

a. Department of Chemistry, Faculty of Science, Yanbian University, Yanji 133002, Jilin, P. R. China;

b. School of Applied Chemistry and Materials, Zhuhai College of Science and Technology, Zhuhai 519041, Guangdong, P. R. China;

c. Laboratory of Theoretical and Computational Chemistry, Institute of Theoretical Chemistry, College of Chemistry, Jilin University, Changchun 130023, Jilin, P. R. China.

Section S1 The Selection and Establishment of Research Model 3

Section S2 Computational Methods 3

S2.1 Density functional theory (DFT) 3

S2.2 Molecular dynamics simulation 3

Section S3 The process of counting clusters and obtaining samples 4

Section S4 Figures and Tables 5

Figure S1. The free region (filled in yellow, showing which regions of the simulated MD box are not occupied by atoms) in the systems simulated by molecular dynamics, isosurface = 0.1. The lower right corner is the three-dimensional coordinate points (x, y, z) of the ten molecules in each system in the microscopic morphology. 5

Figure S2. The probability of occurrence of the value of each charge transfer amount of D_1→A, D_2→A, and D_1→D_2, showing a scatter distribution fitted according to the bar graph in **Figure 5**. The X axis represents the intermolecular net charge transfer amount (|e|), the Y axis represents the percent of occurrences of each charge transfer amount. Color code: purple indicates D_1→A path, orange indicates D_2→A path, green indicates D_1→D_2 path. 6

Figure S3. The radial distribution function of the center of (a) BDT@BDT and (b) C70@C70, (c) stacking diagram of C70 group of $PC_{71}BM$ on the different groups of donor molecule, eg. C70@BDT indicates that C70 is stacked on the BDT unit of donor.. 7

Figure S4. Probability statistics of packing orientations in ternary blends. In the order from left to right, each column of columns represents the ternary of DT:DTE(0.1):$PC_{71}BM$, DT:DTE(0.9):$PC_{71}BM$, DT:P3HT(0.1):$PC_{71}BM$ and DT:P3HT(0.9):$PC_{71}BM$ systems. The number on the top of the column indicates the ratio of the packing orientations between each two molecules to the whole. 7

Figure S5. The energies of CT states, the X-axis (Excited states) corresponds to the calculated 20 excited states, the color represents the oscillator strength of the CT state with the purple→red representing 0→2.2 eV. 8

Table S1. The center of mass (Å) between the donors (BDT@BDT) or acceptors (C70@C70).....8

Section S1 The Selection and Establishment of Research Model

In our previous work, we explored T-OSCs including P3HT:SMPV1:$PC_{71}BM$ and DR3TBDTT:DR3TBDTT-E:$PC_{71}BM$, it was proved that the third component has two effects, which mainly depend on the skeleton similarity between donor and the third component. Based on this point, we found that SMPV1 and DR3TBDTT have the same molecular structure after substituting the side chain with methyl group. But due to the different proportion of the molecule in different systems, it plays different roles in the two systems. That is, when the molecule is used as the main donor, the similar skeletons make the molecule act as the sensitizer and participate in the charge transfer under the cascade energy level; when as a guest donor (the third component), it's a relay station, which could generate excitons, but difficult to participate in the charge generation. It is misleading and unclear of the extent to which skeleton similarity and proportion affect the role of the third component. Therefore, these two groups of molecules were selected and extended to four groups according to doping ratio.

Section S2 Computational Methods

S2.1 Density functional theory (DFT)

The molecular structures of monomers were optimized by the PBE0/6-31G(d,p) level,[1-3] and the ternary blends were optimized using the CAM-B3LYP/6-31G(d,p) with D3 dispersion to characterize the long-range charge transfer excitation properties.[4, 5]

S2.2 Molecular dynamics simulation

MD method was used to simulate the film morphology of the research system using GROMACS (v. 2018.4) software package.[6] The general AMBER force field (GAFF) is used to generate atomic types and intramolecular and intermolecular interaction parameters for small molecules.[7] The force field parameters were generated at the HF/6-31G(d) level to carry out the atomic partial charge of the molecule through the Restricted Electrostatic Potential (RESP) fitting method.[8] Under the three-dimensional periodic boundary conditions (PBC), MD simulation was run using leap-frog integrator with time step of 2 fs through canonical (NVT) ensemble balance. Temperature and pressure were controlled by Velocity Rescaling thermostat and Berendsen Barostat, respectively. The sum of van der Waals interaction and real space electrostatic interaction is spherical cut-off of 1.2 nm, and the long range electrostatic interaction is solved using the Particle Mesh Ewald (PME) solver. The temperature and pressure were relaxed to 298 K and 1 bar by the pre-balancing process of 1ns thermal annealing, and the stable and balanced morphology was obtained by simulating the finished product with 50 ns.

The free region is visualized by MD simulation to observe the region that is not occupied by atoms under the micro-morphology of the blends. In order to compare the influence of skeleton similarity and proportion, original

binary blending systems were introduced, as shown in **Figure S1**. It was obvious that there is a certain sparse region (yellow fill range) in four ternary systems, and the spatial region is similar. Subsequently, according to the calculation principle of free volume, the spatial volume of the free region was quantified. Free volume is defined as (or calculated by) the number of all unoccupied lattices multiplied by the lattice volume. Except the occupied lattice, which is considered as the distance of a lattice from any atom is within the van der Waals radius of that atom, the rest is unoccupied. The increase of free volume indicates that the system is compact and there is more contact between donors and acceptors.

Section S3 The process of counting clusters and obtaining samples

Taking the third component or host donor (only ten) of each of the system as the original point, all reasonable fullerene acceptors with potential for stacking with the third component were counted in accordance with the appropriate stacking distance of 3.5-4.0 Å between fullerenes and the donors. Similarly, the next step is to get the donor molecule at the corresponding distance for each fullerene molecule. Ten clusters, i.e. 1clu.~10clu., could be obtained by summing up the donor and fullerene molecules around each third component into a small whole. Each cluster contains only one third component.

DT:DTE(0.1):$PC_{71}BM$, DT:DTE(0.9):$PC_{71}BM$, DT:P3HT(0.1):$PC_{71}BM$ and DT:P3HT(0.9):$PC_{71}BM$ ternary systems obtained 42, 42, 29, 46 samples respectively. According to the work of Wei's group, the classification standard of molecular orientation is defined,[9] Face-on stacking orientation is defined as the center of mass less than 8 Å, and the angle between fullerene and the plane of a conjugated group on the donor molecule is less than 30°; For Edge-on, the center of mass is 8~9 Å and fullerenes are on one side of the main chain; other accumulation orientation is defined as Slipped.

Section S4 Figures and Tables

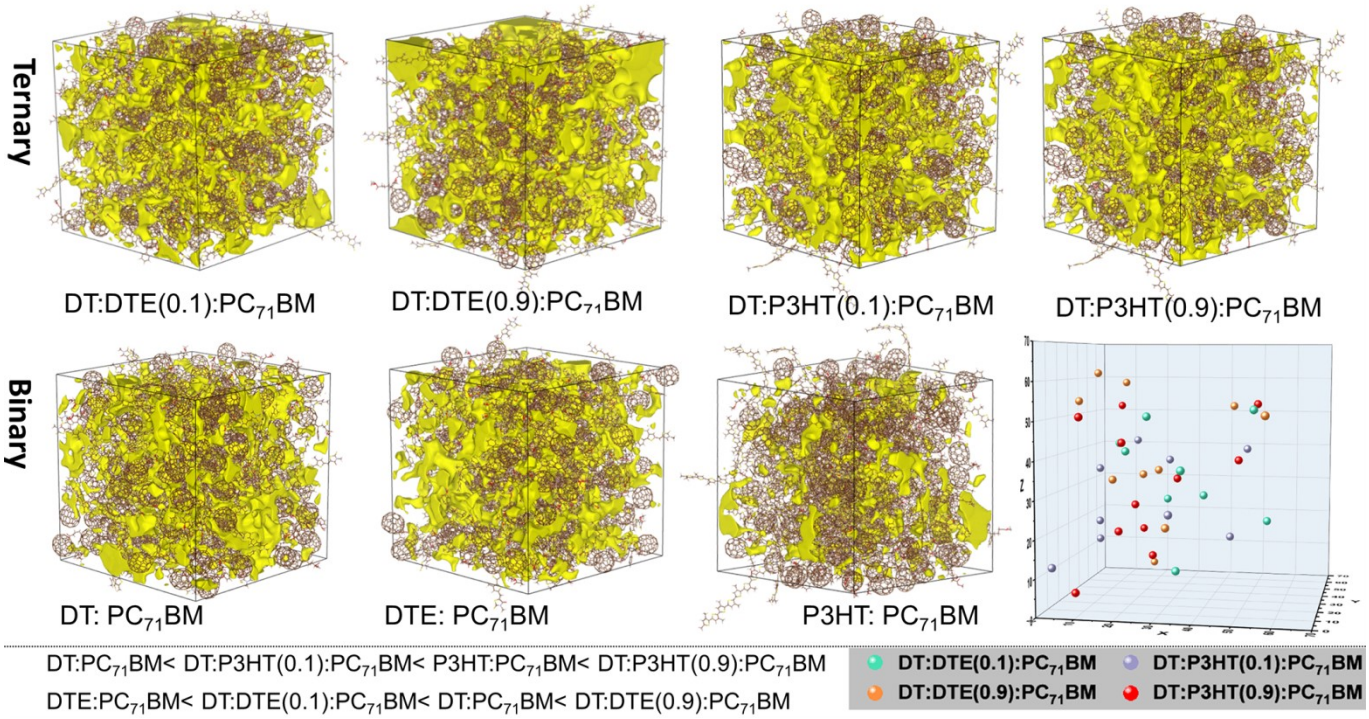

Figure S1. The free region (filled in yellow, showing which regions of the simulated box are not occupied by atoms) in the systems simulated by molecular dynamics, isosurface = 0.1. The lower right corner is the three-dimensional coordinate points (x, y, z) of the ten molecules in each system in the microscopic morphology.

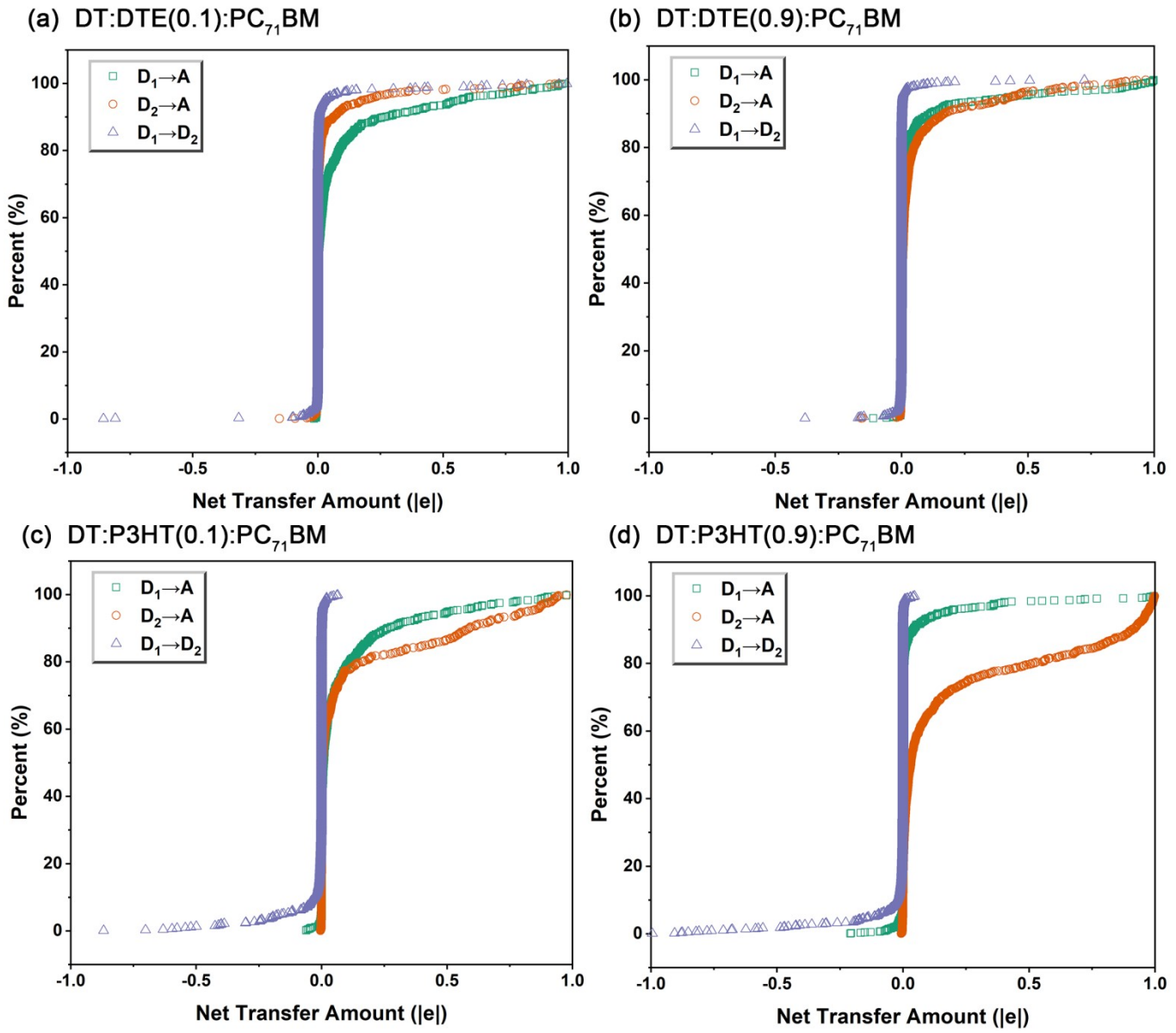

Figure S2. The probability of occurrence of the value of each charge transfer amount of D_1→A, D_2→A, and D_1→D_2, showing a scatter distribution fitted according to the curve in **Figure 2**. The X axis represents the intermolecular net charge transfer amount (|e|), the Y axis represents the percent of occurrences of each charge transfer amount. Color code: purple indicates D_1→A path, orange indicates D_2→A path, green indicates D_1→D_2 path.

The comparison result needs to be judged conjunctively according to the position of the peak in Figure 2 and the slope in Figure S2 respectively. On the one hand, a larger |e| should have the characteristics of a peak shift (of curve) to the positive direction of X axis, that is, the highest peak of the Gaussian fitting curve approaches 1. It is necessary to find the corresponding amount |e| (X-axis value) according to the highest peak (Y-axis value is the largest), and then compare the amount in each system. On the other hand, it should have a smaller slope in Figure S2, because the smaller the slope, the more likely the CT path exists.

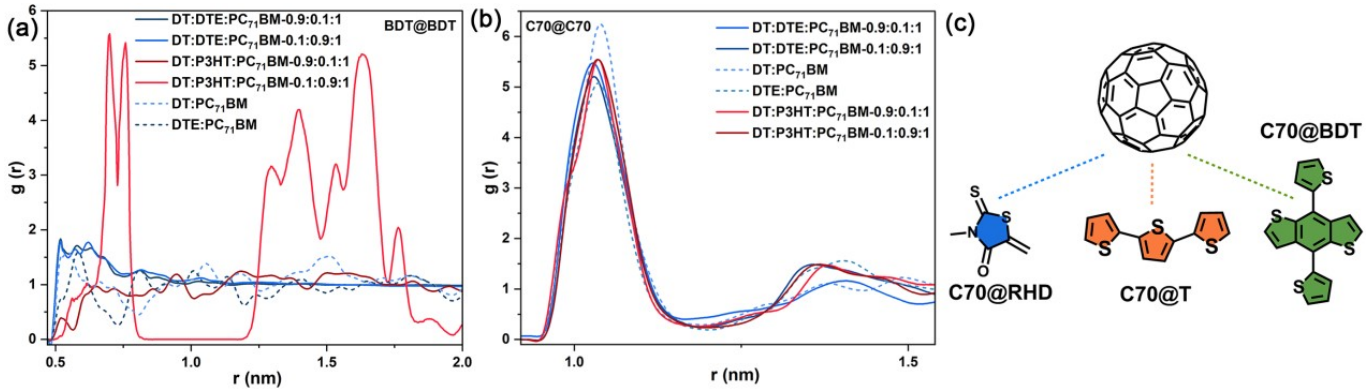

Figure S3. The radial distribution function (RDF) of the center of mass (COM) of (a) BDT@BDT and (b) C70@C70. (c) Stacking diagram of C70 group of $PC_{71}BM$ on the different groups of donor molecule, eg. C70@BDT indicates that C70 is stacked on the BDT unit of donor.

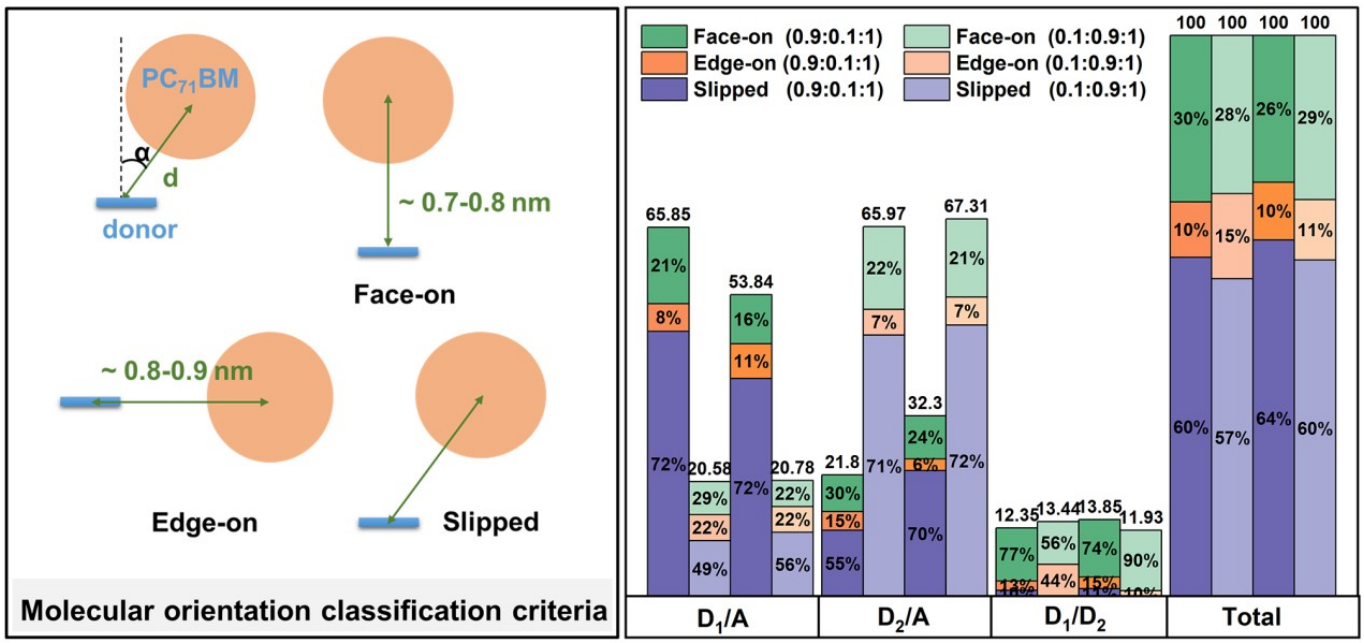

Figure S4. Left figure represents the molecular orientation classification criteria. Right figure represents the probability statistics of packing orientations in ternary blends. In the order from left to right in the right figure, each column of columns represents the ternary of DT:DTE(0.1):$PC_{71}BM$, DT:DTE(0.9):$PC_{71}BM$, DT:P3HT(0.1):$PC_{71}BM$ and DT:P3HT(0.9):$PC_{71}BM$ systems. The number on the top of the column indicates the ratio of the packing orientations between each two molecules to the whole.

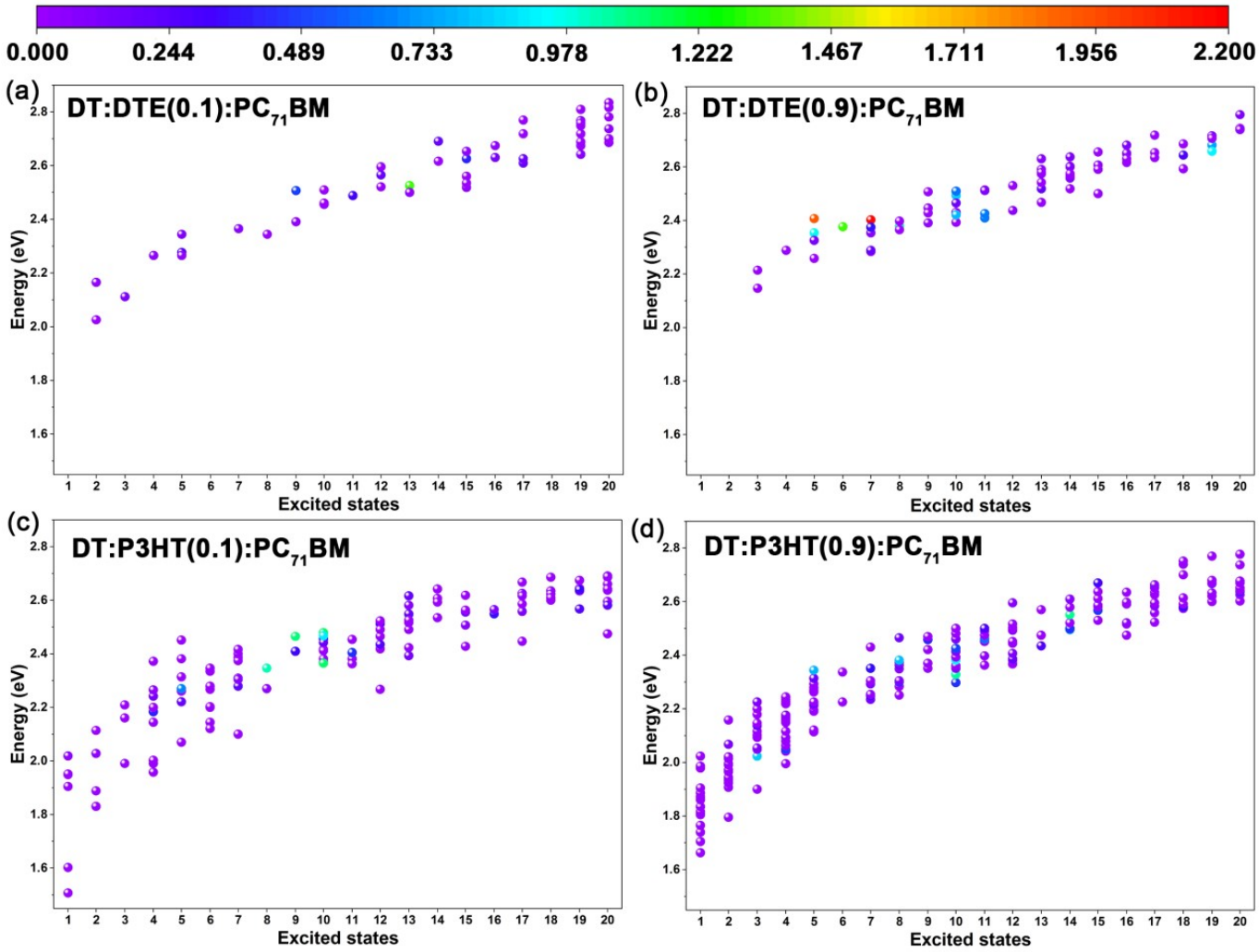

Figure S5. The energies (eV) of CT states, the X-axis (Excited states) corresponds to the calculated 20 excited states, the color represents the oscillator strength of the CT state with the purple→red representing 0→2.2 eV.

Table S1. The center of mass (Å) between the donors (BDT@BDT) or acceptors (C70@C70)

	DT:DTE(0.1):$PC_{71}BM$	DT:DTE(0.9):$PC_{71}BM$	DT:P3HT(0.1):$PC_{71}BM$	DT:P3HT(0.9):$PC_{71}BM$	DT:$PC_{71}BM$	DTE:$PC_{71}BM$
BDT@BDT	8.96	9.10	5.22	7.00	5.50	5.84
C70@C70	10.28	10.30	10.36	10.34	10.40	10.36

References

1. L. Zhang, K. Pei, M. Yu, Y. Huang, H. Zhao, M. Zeng, Y. Wang and J. Gao, *J. Phys. Chem. C*, 2012, **116**, 26154-26161.
2. D. Jacquemin, E. A. Perpète, G. E. Scuseria, I. Ciofini and C. Adamo, *J. Chem. Theory Comput.*, 2008, **4**, 123-135.
3. D. Jacquemin, J. Preat, V. Wathelet, M. Fontaine and E. A. Perpète, *J. Am. Chem. Soc.*, 2006, **128**, 2072-2083.
4. T. Yanai, D. P. Tew and N. C. Handy, *Chem. Phys. Lett.*, 2004, **393**, 51-57.
5. M.-Y. Li, H. Yin, M.-Y. Sui, F. Wang, Y.-H. Liu and G.-Y. Sun, *Int. J. Quantum. Chem.*, 2019, **119**, e25938.
6. B. Hess, C. Kutzner, D. van der Spoel and E. Lindahl, *J. Chem. Theory Comput.*, 2008, **4**, 435-447.

7. G. Han, Y. Guo, X. Ma and Y. Yi, *Sol. RRL*, 2018, **2**, 1800190.
8. C. I. Bayly, P. Cieplak, W. Cornell and P. A. Kollman, *J. Phys. Chem. C*, 1993, **97**, 10269-10280.
9. Z. Wang, G. Han, L. Zhu, Y. Guo, Y. Yi, Z. Shuai and Z. Wei, *Phys. Chem. Chem. Phys*, 2018, **20**, 24570-24576.